HHS Public Access

Author manuscript

Nanoscale. Author manuscript; available in PMC 2016 December 03.

Published in final edited form as:

Nanoscale. 2016 March 28; 8(12): 6542–6554. doi:10.1039/c6nr00398b.

Anti-atherogenic Effect of Trivalent Chromium-loaded CPMV Nanoparticles in Human Aortic Smooth Muscle Cells under Hyperglycemic Conditions *in vitro*

Rituparna Ganguly[1,2], **Amy M. Wen**[3], **Ashley B. Myer**[1], **Tori Czech**[1], **Soumyadip Sahu**[1,2], **Nicole F. Steinmetz**[3,4,5,6,7], and **Dr. Priya Raman**[1,2]

Priya Raman: praman@neomed.edu

[1]Department of Integrative Medical Sciences, Northeast Ohio Medical University, 4209 State Route 44, Rootstown, OH 44272-0095, USA

[2]School of Biomedical Sciences, Kent State University, Kent, OH, USA

[3]Department of Biomedical Engineering, 10990 Euclid Avenue, Case Western Reserve University, Cleveland OH, USA

[4]Department of Radiology, 10990 Euclid Avenue, Case Western Reserve University, Cleveland OH, USA

[5]Department of Materials Science and Engineering, 10990 Euclid Avenue, Case Western Reserve University, Cleveland OH, USA

[6]Department of Macromolecular Science and Engineering, 10990 Euclid Avenue, Case Western Reserve University, Cleveland OH, USA

[7]Case Comprehensive Cancer Center, 10990 Euclid Avenue, Case Western Reserve University, Cleveland OH, USA

Abstract

Atherosclerosis, a major macrovascular complication associated with diabetes, poses tremendous burden on national health care expenditure. Despite extensive efforts, cost-effective remedies are unknown. Therapies for atherosclerosis are challenged by lack of targeted drug delivery approach. Toward this goal, we turn to a biology-derived drug delivery system utilizing nanoparticles formed by the plant virus, Cowpea mosaic virus (CPMV). The aim herein is to investigate the anti-atherogenic potential of the beneficial mineral nutrient, trivalent chromium, loaded CPMV nanoparticles in human aortic smooth muscle cells (HASMC) under hyperglycemic conditions. A non-covalent loading protocol is established yielding $CrCl_3$-loaded CPMV (CPMV-Cr) carrying 2,000 drugs per particle. Using immunofluorescence microscopy, we show that CPMV-Cr is readily uptaken by HASMC *in vitro*. In glucose (25 mM)-stimulated cells, 100 nM CPMV-Cr inhibits HASMC proliferation concomitant to attenuated proliferating cell nuclear antigen (PCNA, proliferation marker) expression. This is accompanied with attenuation in high glucose-induced phospho-p38 and pAkt expression. Moreover, CPMV-Cr inhibits expression of pro-inflammatory cytokines, transforming growth factor-β (TGF-β) and nuclear factor kappa-light-chain-enhancer

Correspondence to: Priya Raman, praman@neomed.edu.

of activated B cells (NF-κB), in glucose-stimulated HASMCs. Finally glucose-stimulated lipid uptake is remarkably abrogated by CPMV-Cr, revealed by Oil Red O staining. Together, these data provide key cellular evidence for an atheroprotective effect of CPMV-Cr in vascular smooth muscle cells (VSMC) under hyperglycemic conditions that may promote novel therapeutic ventures for diabetic atherosclerosis.

Graphical abstract

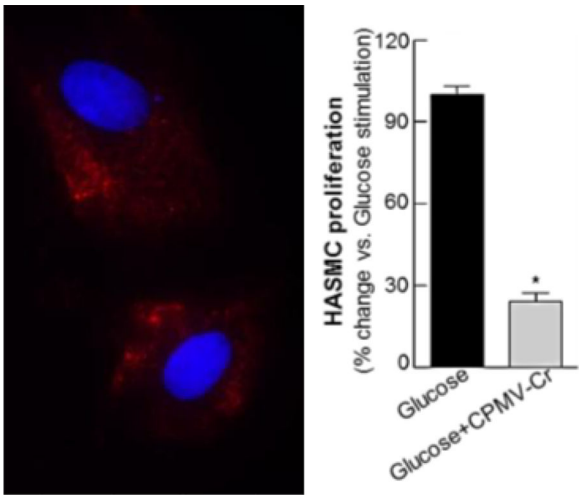

Novel trivalent chromium-loaded cowpea mosaic virus nanoparticles exhibit atheroprotective effect in vascular smooth muscle cells in a diabetic milieu.

Keywords

CPMV nanoparticles; trivalent chromium; vascular smooth muscle cells; hyperglycemia; anti-atherogenic effect

Introduction

Vascular disease accounts for increased morbidity and mortality in diabetic patients. Atherosclerosis characterized by excessive lipid deposition in the vessel wall leads to progressive luminal narrowing, limiting blood flow to target organs and triggering a multitude of cardiovascular complications.[1] Diabetic patients have two- to four-fold greater risks of developing atherosclerotic complications.[2–4] Despite significant advances, cost-effective strategies to alleviate risks of macrovascular complications in diabetes have remained elusive. Trivalent chromium (Cr^{3+}) is a mineral nutrient long acclaimed for its beneficial glycemic and cardiovascular effects.[5–11] Diabetic patients have low tissue Cr^{3+} levels, and numerous studies have indicated that suboptimal Cr^{3+} intake leads to elevated blood glucose, insulin and lipid levels as well as increased cardiovascular risks.[12] *In vivo* and *in vitro* studies have shown that Cr^{3+} inhibits lipid peroxidation and attenuates secretion of pro-inflammatory cytokines including tumor necrosis factor-alpha (TGF-α), interleukin-6 (IL-6), monocyte chemoattractant protein-1 (MCP-1) and C-reactive protein (CRP),[13–16] suggesting a putative role in lowering risks of vascular inflammation in diabetes. We

recently reported that Cr^{3+} downregulates a potent pro-atherogenic protein thrombospondin-1 (TSP-1) expression and attenuates reactive oxygen species (ROS) formation coupled with an anti-proliferative effect in glucose-stimulated human aortic smooth muscle cells (HASMC) *in vitro.*[17] These data lend support to the notion that Cr^{3+} modulates abnormal vascular smooth muscle cell (VSMC) function under hyperglycemic conditions, bearing significantly upon diabetic vascular disease.

Current therapies for diabetic atherosclerosis are not targeted to the site of disease and therefore have major limitations coupled with reduced efficacy. While Cr^{3+} is a relatively inexpensive nutraceutical with low mutagenic potential,[18–20] systemic administration at dosages of 2–3 mg/kg is considered toxic.[18, 21, 22] Thus, tissue-targeted drug delivery systems are needed to overcome the dose-limiting toxicities. Toward this goal, we turn to a biology-inspired nanotechnology approach; specifically we are using nanoparticles derived from a plant virus.

Many novel types of nanomaterials are in the developmental pipeline, and viruses have played a special role because they can be considered as Nature's delivery systems. Based on their highly symmetrical and well-defined structures, plant viruses have advantages compared to their synthetic counterparts and they are favored over mammalian viruses owing to their higher safety profile in humans.[23] The 30 nm-sized Cowpea mosaic virus (CPMV) is such a plant virus-derived nanoparticle, extensively studied for its biomedical applications in the field of cancer and cardiovascular medicine.[24–28] The structure of CPMV is known to near atomic resolution, with well-established inside-out surface chemistry.[29] CPMV is biocompatible and biodegradable allowing intravenous or oral delivery as purified nanoparticles or edible plant tissue,[30] administered at doses of up to 100 mg/kg body weight without signs of toxicity[31, 32] rendering it a suitable platform for drug delivery.

While bacteriophages and other plant viruses are also being actively studied, with some examples in cancer therapy[33–35] and tissue engineering,[36–38] previous studies have shown that CPMV nanoparticles naturally interact with surface-expressed vimentin;[27, 39, 40] this natural targeting mechanism can be utilized for disease-specific delivery. Moreover, earlier studies have reported that CPMV nanoparticles target atherosclerotic lesions and correlate with increased cell surface vimentin expression in lesions.[26] The goal of the present study was to develop and investigate the anti-atherogenic potential of chromium chloride ($CrCl_3$)-loaded CPMV nanoparticles (CPMV-Cr) in primary HASMC cultures under hyperglycemic conditions *in vitro*.

Results

Sustained Cr^{3+} Release from CPMV Nanoparticles

Taking advantage of the RNA encapsulated within CPMV, it has previously been shown that gadolinium (Gd^{3+}) and terbium (Tb^{3+}) ions can be loaded through high affinity interactions with the RNA.[41] Since Cr^{3+} has a comparable charge, we hypothesized a similar method could be used for infusing chromium within CPMV. 5 mg/mL CPMV was incubated with 50 mM $CrCl_3$ (~60,000 equivalents) in 50 mM HEPES buffer containing 30 mM ethylenediaminetetraacetic acid (EDTA) and dialyzed against 10 mM EDTA in 10 mM

HEPES. The Cr^{3+} concentration over 7 days was determined by Inductively Coupled Plasma Optical Emission Spectroscopy (ICP-OES), shown in Figure 1A. It was observed that after 3 days, a stable loading value of 2000 +/− 20% was reached, which is significantly higher than values of around 80 achieved previously with Gd^{3+} and Tb^{3+}.[41] For subsequent studies, CPMV-Cr samples were purified over 3 days and characterized using ICP-OES before use. Particle morphology examined by transmission electron microscopy (TEM) revealed that the particles remained intact and incubation with $CrCl_3$ did not destabilize the particles (Figure 1B).

Uptake of $CrCl_3$-loaded CPMV by HASMC

To confirm the cellular uptake of CPMV-Cr, primary HASMC cultures were treated with 25 mM glucose and incubated with 100 nM $CrCl_3$-loaded CPMV. Staining was achieved using an anti-CPMV antibody followed by secondary staining. Immunofluorescence microscopy showed a significant increase in CPMV staining, as revealed by enhanced red cytoplasmic staining. In contrast, no cytoplasmic staining was detected when cells were incubated in the absence of anti-CPMV antibody. These data clearly demonstrate HASMC targeting and cellular delivery of CPMV (Figure 2).

$CrCl_3$-loaded CPMV Inhibits HASMC Proliferation under Hyperglycemic Conditions

We recently reported that Cr^{3+} inhibits high glucose-induced HASMC proliferation *in vitro*.[17] To investigate whether these effects are preserved in cells incubated with $CrCl_3$-loaded CPMV nanoparticles, primary HASMCs incubated with 25 mM glucose in presence or absence of 100 nM $CrCl_3$-loaded CPMV were used in a cell proliferation assay. As shown in Figure 3A, CPMV-Cr significantly attenuated high glucose-induced HASMC proliferation. Specifically in glucose-stimulated cells, HASMC proliferation was inhibited by 76% following incubation with CPMV-Cr (vs. glucose alone, $p \leq 0.05$). Consistent with these results, immunoblotting experiments demonstrated that CPMV-Cr decreased PCNA expression, a marker of cellular proliferation, in glucose-stimulated HASMC. Densitometric quantification revealed that while high glucose increased PCNA expression by 25% compared to untreated controls, incubation with CPMV-Cr significantly attenuated glucose-induced PCNA expression (Figure 3B, 41% vs. glucose alone, $p = 0.026$). Next, to elucidate the signaling mechanism responsible for this anti-proliferative response, the effect of CPMV-Cr on the expression of key signaling mediators of VSMC proliferation was assessed. Briefly, glucose-stimulated HASMCs treated with or without CPMV-Cr were subjected to immunoblotting using antibodies specific for phospho-p38, total-p38, phospho-Akt and total-Akt. $CrCl_3$-loaded CPMV attenuated activation of both p38 and Akt protein expression in glucose-stimulated cells. Specifically, while 25 mM glucose increased phospho-p38 and pAkt expression in primary HASMC cultures (76% and 66.8%, respectively), there was a statistically significant decrease in protein expression of both phospho-p38 and pAkt in cells incubated with $CrCl_3$-loaded CPMV compared to cells treated with glucose alone (Figure 3C, 3D, 49% and 59.3%, respectively, $p = 0.004$).

$CrCl_3$-loaded CPMV Attenuates the Expression of Pro-inflammatory Cytokines in HASMC under Hyperglycemic Conditions

Consistent with our earlier reports studying the effects of $CrCl_3$,[17] incubation with $CrCl_3$-loaded CPMV significantly inhibited the pro-atherogenic protein thrombospondin-1 (TSP-1) expression in glucose (25 mM)-stimulated HASMC cultures *in vitro*. Specifically, while high glucose increased TSP-1 expression by 2.9-fold compared to untreated controls, CPMV-Cr remarkably attenuated TSP-1 expression in glucose-stimulated HASMCs (Figure. 4A, 76% vs. glucose alone, $p = 0.04$). Next, the effect of CPMV-Cr on the expression of pro-inflammatory cytokines, TGF-β and NF-κB, was assessed. Earlier studies have reported that high glucose upregulates TGF-β expression in VSMC as early as after 6 h of stimulation.[42] Accordingly, primary HASMCs were treated with 25 mM glucose in presence or absence of CPMV-Cr and incubations were continued for 6–24 h. A significant increase in TGF-β expression was observed at both 6 h (data not shown) and 12 h of glucose stimulation and this effect was somewhat maintained up to 24 h (data not shown). Under similar experimental conditions, incubation with CPMV-Cr inhibited glucose-induced TGF-β expression. Quantification of immunoblotting images showed that while TGF-β protein expression was increased by 2.5-fold following 12 h glucose stimulation, there was a significant decrease in high glucose-induced TGF-β expression in response to CPMV-Cr (Figure 4B, 68.9% vs. glucose alone, $p = 0.015$). Similarly, high glucose increased NF-κB protein expression in HASMC *in vitro* and this effect was markedly attenuated by incubation with CPMV-Cr. Densitometric quantification of immunoblots revealed that while high glucose increased NF-κB expression by 2.2-fold compared to untreated cells, incubation with CPMV-Cr significantly inhibited NF-κB expression in glucose-stimulated HASMC (Figure 4C, 69.4% compared to cells treated with glucose alone, $p = 0.005$).

$CrCl_3$-loaded CPMV Inhibits Uptake of ox-LDL in Glucose-stimulated HASMC

To determine the effect of $CrCl_3$-loaded CPMV on lipid uptake by HASMCs under hyperglycemic conditions, primary HASMC cultures stimulated with 25 mM glucose with or without $CrCl_3$-loaded CPMV were incubated with oxidized-low density lipoprotein (ox-LDL) and cellular lipid uptake was detected microscopically using Oil Red O staining. As shown in Figure 5, a significant increase in Oil Red O staining indicative of enhanced lipid uptake was observed in cells incubated with glucose alone. In contrary, CPMV-Cr remarkably abrogated high glucose-induced lipid uptake, revealed by reduced Oil Red O staining. Quantification of Oil Red O staining intensity depicted 3.36-fold increase ($p = 0.002$) in ox-LDL uptake in glucose-treated HASMC; CPMV-Cr, on the other hand, reduced lipid staining by ~70% in glucose-stimulated cells as compared to HASMCs treated with glucose alone ($p = 0.001$). Interestingly, CPMV nanoparticles in the absence of bound $CrCl_3$ did not have any effect on the cellular uptake of ox-LDL in glucose-stimulated HASMC cultures (data not shown).

Discussion

The present study demonstrates novel anti-atherogenic effects of $CrCl_3$-loaded CPMV nanoparticles in primary HASMC cultures in a diabetic milieu *in vitro*. These data suggest a potential application of CPMV nanoparticles as a suitable drug delivery platform for the

mineral nutrient trivalent chromium in VSMCs. Accumulating literature highlight the utility of CPMV in a number of biomedical applications and nano-biotechnology including development of vaccines,[43] imaging agents,[25, 28, 44] therapeutics[45] and chemical scaffolds.[46–48] CPMV and other plant virus-based scaffolds provide unique advantages for applications in drug delivery: a particular advantage is their propagation in plants affording scalability and high degree of quality control and assurance. Being genetically encoded, these plant virus-based nanomaterials form highly monodisperse products with predictable surface morphologies. Furthermore, since plant viruses do not infect but enter mammalian cells, they provide a unique opportunity for intracellular drug delivery. CPMV, in particular, provides an interesting and unique platform because of its natural targeting to cells and tissues expressing surface vimentin.[39, 49]

Indeed, earlier studies have reported the ability of CPMV nanoparticles to be internalized by multiple cell types including cancer cells, endothelial cells and macrophages; in each case, cell targeting and uptake correlated with surface vimentin expression.[27, 45, 50] Vimentin is a ubiquitous cytoskeletal component involved in basic cellular processes such as cell adhesion, migration, proliferation, cell-cell interactions as well as gene expression and signal transduction mechanisms.[51] In its surface-expressed form, vimentin is thought to mediate endothelial interactions with circulating blood cells and migrating cells.[52] Animal studies using the $LDLR^{-/-}$ mouse model of atherosclerosis demonstrated increased localization of CPMV nanoparticles in endothelial cells and macrophages within atherosclerotic lesions *in vivo*; again, CPMV targeting to the site of disease was correlated with surface vimentin expressed at the atherosclerotic lesion. On the other hand, in the absence of lesions, CPMV failed to penetrate the intact endothelium and remained associated with the endothelial cell layer in the non-lesion aorta.[50] Although previous studies have demonstrated a rapid uptake of CPMV by a diverse group of cells *in vivo* and *in vitro*, interaction of CPMV with VSMC has not been previously examined. The present study provides the first evidence that CPMV nanoparticles are readily taken-up by primary HASMC cultures under diabetic conditions *in vitro*. Previous studies have indicated vimentin as a major intermediate filament protein expressed on VSMC that play a role in organization of the cytoskeletal framework of these cells.[53] Moreover, surface-expressed vimentin on VSMCs have also been reported to possess O-GlcNAc-binding lectin-like properties.[54] Accordingly, uptake of CPMV by HASMCs observed in this work suggests a role of cell-surface vimentin, as previously reported for other cell types.

Smooth muscle cells (SMC) are integral cells in the vessel wall that regulate the tone and contractility of the vasculature. In a healthy blood vessel, SMCs are localized within the medial layer of the vascular wall in a quiescent, contractile state. In response to pro-atherogenic stimuli, SMCs undergo a phenotypic switching to a synthetic, proliferative phase, which predominantly resides in the intimal layer of the vessel wall.[55, 56] Diabetic patients have an increased propensity for aberrant VSMC migration and proliferation,[57] a hallmark of the synthetic SMC phenotype. Deregulation of VSMC phenotype from a differentiated to de-differentiated state, characterized by enhanced secretory and proliferative properties with low levels of contractile gene expression, is a major pathophysiological trigger for initiation and progression of atherosclerosis.[55, 58] We recently reported that Cr^{3+} inhibits high glucose-induced HASMC proliferation that is specific for

glucose-stimulated conditions as opposed to serum-stimulation *in vitro*; moreover, this anti-proliferative effect was independent of the anionic ligand (chloride or picolinate) bound to Cr^{3+}.[17] Consistent with these data, the present study demonstrates a strong anti-proliferative response to supplementation with $CrCl_3$-loaded CPMV nanoparticles in glucose-stimulated primary HASMC cultures. Although multiple studies have suggested beneficial outcomes of Cr^{3+} supplementation in cardiovascular disease and dysregulated glycemic health, growing reports emphasize that long-term use of Cr^{3+} can result in GI disturbances, liver problems and impaired coordination or cognition; high cellular concentrations can further lead to DNA damage.[22] Moreover, clinical trials using Cr^{3+} have yielded mixed results possibly confounded by the use of oral dose of Cr^{3+} viewed as being 'too low' and poor or inconsistent bio-distribution profiles of Cr^{3+} formulations.[59, 60] To this end, the current work revealing an inhibitory effect of $CrCl_3$-loaded CPMV on HASMC proliferation under hyperglycemic conditions highlight an enhanced potential of CPMV nanoparticles as an ideal platform for lesion-targeted delivery of Cr^{3+}.

Extensive literature demonstrates that the p38-MAPK pathway and AKT family of serine threonine kinases are critical regulators of cell growth and proliferation.[61, 62] Previous studies have reported that activation of p38-MAPK following vascular injury promotes neointimal hyperplasia mediated via release of pro-inflammatory and fibroproliferative cytokines and growth factors.[63] Multiple lines of evidence suggest that p38-MAPK pathway plays a pivotal role in diverse cellular processes including cell migration, proliferation, differentiation and cell cycle regulation. Both *in vivo* and *in vitro* studies have shown that selective inhibition of p38-MAPK attenuates aberrant VSMC proliferation limiting neointimal growth and abnormal vascular remodeling, characteristic of atherosclerosis.[61, 63, 64] Earlier studies have also shown that activation of Akt and p38-MAPK by high glucose initiates downstream signaling cascades that mediate upregulation of several cell cycle-related genes including cyclin D, cyclin E and PCNA.[65] In accordance with these earlier reports, the current findings that CPMV-Cr inhibits phospho-p38-MAPK and phospho-AKT expression in glucose-stimulated HASMCs suggest that ablation of VSMC growth response and cell cycle-regulated pathways may serve as important targets of $CrCl_3$-loaded CPMV nanoparticles under hyperglycemic conditions.

Atherosclerotic lesions typically have an enhanced inflammatory milieu. Upregulation of pro-inflammatory chemokines such as MCP-1 triggers migration and activation of monocytes into macrophages within the subendothelial space of the vessel wall; mature macrophages capable of ingesting atherogenic lipids, in turn contribute to plaque evolution.[66] Previous studies have shown that supplementation with chromium dinicocysteinate *in vivo* significantly reduced CRP, MCP-1 and ICAM-1 levels in Zucker diabetic fatty rats.[67] Additionally, *in vivo* administration of chromium niacinate and chromium picolinate lowered blood levels of TGF-α, IL-6 and CRP coupled to reduced triglyceride and cholesterol concentration in streptozotocin-treated diabetic rats.[16] Furthermore, *in vitro* studies using isolated human blood mononuclear cells and U937 monocytes have shown that chromium chloride and chromium niacinate inhibit TGF-α, IL-6, IL-8 and MCP-1 secretion in glucose-stimulated cells.[13, 15] We recently reported that Cr^{3+} downregulates a potent pro-atherogenic protein thrombospondin-1 (TSP-1) expression in glucose-stimulated HASMC cultures and this effect was associated with its anti-

proliferative response.[17] Consistent with these earlier findings, the current work demonstrated that $CrCl_3$-loaded CPMV nanoparticles inhibit high glucose-induced TSP-1 expression in HASMCs *in vitro*. TSP-1 belongs to a family of extracellular matrix proteins that regulate cell-cell and cell-matrix interactions.[68, 69] Earlier studies have reported increased TSP-1 expression in the injured wall[70, 71] and early-stage atherosclerotic lesions,[72] with enhanced expression in VSMC,[73] and have implicated a role of TSP-1 in restenosis.[74] Diabetic patients and diabetic animal models show enhanced TSP-1 expression;[75, 76] moreover, an upregulation of TSP-1 expression was also reported in vascular cells exposed to high glucose *in vitro*.[76, 77] Notably in the current work, TSP-1 downregulation was accompanied with attenuation in high glucose-induced TGF-β expression by CPMV-Cr. Numerous *in vitro* and *in vivo* studies have reported that TSP-1 is a critical endogenous activator of TGF-β, a potent chemotactic pro-inflammatory cytokine.[78] TGF-β, a multifunctional polypeptide, regulates diverse cellular processes including cell growth, proliferation, differentiation, cell motility and apoptosis. Earlier studies have linked TGF-β with a multitude of diabetic complications including macrovascular disease and restenosis, diabetic nephropathy and diabetic cardiomyopathy.[79, 80] Elevated TGF-β expression was found in diabetic patients, diabetic animal models as well as in a number of cell types (mesangial cells, VSMC) exposed to high glucose *in vitro*.[78, 81] Previous studies have also demonstrated that Cr^{3+} *in vivo* inhibits the expression of NF-κB, a key transcription factor that mediates inflammatory and immune responses, in Zucker diabetic fatty liver.[67] Earlier work suggests under certain pathological conditions, there exist direct correlations between the inflammatory response and NF-κB activation. Additionally, *in vitro* and *in vivo* studies demonstrate that NF-κB inhibition can dramatically abrogate development of atherosclerotic lesions modulated via attenuation of inflammatory and VSMC proliferative responses.[82] Cogent to these reports, the present study revealing attenuation of TSP-1, TGF-β and NF-κB expression in glucose-stimulated VSMC suggest a protective role of $CrCl_3$-loaded CPMV nanoparticles in development of fibroproliferative vascular remodeling associated with diabetes.

Excessive accumulation of low density lipoproteins (LDLs) within the subendothelial spaces of the arterial vessel wall is a hallmark of atherosclerosis. While macrophages are the predominant cell-type associated with lipid uptake in the arterial intima, growing evidence demonstrate an increased ability of VSMC to incorporate aggregated LDLs, in turn contributing to foam cell formation.[83] Earlier studies have shown that VSMCs express LDL receptor-related protein 1 (LRP1) that is capable of binding and internalizing aggregated LDLs, resulting in increased cholesteryl ester accumulation in VSMCs.[84] LRP1 was initially identified as an endocytosis-mediated receptor for many ligands including thrombospondins, plasma lipoproteins such as apoE-enriched VLDL, lipoprotein lipase and lipoprotein lipase-triglyceride rich lipoprotein complexes.[85] Previous studies have demonstrated that hypercholesterolemia upregulates LRP1 expression on VSMC, mediating enhanced cholesterol accumulation within these cells, in turn modulating collagen assembly and proteoglycan composition in VSMCs.[86] Recent studies further indicate that defects in LRP1 expression in the vascular wall may promote atherosclerosis via increased VSMC proliferation.[85] In the context of these earlier reports, findings from the present study that $CrCl_3$-loaded CPMV nanoparticles inhibit high glucose-induced lipid uptake in VSMC

prompt us to speculate that these effects may be mediated via modulation of LRP-1 by CPMV-Cr. Interestingly, CPMV nanoparticles in the absence of any bound Cr^{3+} did not have any effect on the expression of pro-inflammatory cytokines and VSMC lipid uptake stimulated by hyperglycemic conditions *in vitro* (data not shown).

Conclusion

In summary, the current study provides the first cellular evidence for important anti-atherogenic effects of $CrCl_3$-loaded CPMV nanoparticles in VSMC under hyperglycemic conditions. Specifically using cell proliferation assay and immunoblotting experiments, we have shown that $CrCl_3$-loaded CPMV nanoparticles inhibit smooth muscle cell proliferation and protein expression of a cell proliferation marker, PCNA, in glucose-stimulated HASMC primary cultures. This anti-proliferative effect of CPMV-Cr was further accompanied with significant attenuation in activation of high glucose-induced p38-MAPK and AKT expression, critical signaling mediators of smooth muscle cell proliferation. In addition, incubation with CPMV-Cr inhibited the expression profiles of pro-atherogenic matricellular protein (TSP-1) and pro-inflammatory cytokines (TGF-β and NF-κB) in HASMC under diabetic milieu, as shown by immunoblotting. Finally, Oil red O staining revealed that supplementation with CPMV-Cr remarkably abrogated high glucose-induced lipid uptake in HASMC cultures. Overall, these data strongly support the notion that CPMV plant virus-based nanoparticles may present a novel platform technology enabling lesion-targeted Cr^{3+} delivery in diabetes, which may promote increased efficacy at reduced dosage while avoiding systemic toxicity. Future *in vivo* studies using an atherosclerotic mouse model of diabetes to determine whether $CrCl_3$-loaded CPMV nanoparticles may facilitate lesion-specific Cr^{3+} delivery and attenuate development of atherosclerotic lesions warrant further investigation. Such studies will set the stage for preclinical development of CPMV-Cr to treat atherosclerotic complications associated with diabetes.

Experimental Section

CPMV Purification and Cr^{3+} Drug Loading

CPMV nanoparticles were purified from *Vigna unguiculata* plants infected by mechanical inoculation using a 0.1 mg/mL solution of CPMV in 0.1 M potassium phosphate buffer. Yields of 1 mg/g of infected leaf material were obtained using established procedures.[87] For chromium loading, 5 mg/mL CPMV was incubated with 50 mM $CrCl_3$ (Sigma Aldrich) and 30 mM ethylenediaminetetraacetic acid (EDTA) in 50 mM HEPES buffer, pH 7 overnight (~60,000-fold molar excess). The sample was then dialyzed against 10 mM HEPES buffer with 10 mM EDTA using 12–14 kDa molecular weight cut-off tubing (Spectrum Laboratories) over 3 days. Some precipitation from the presence of NaOH in the buffer was observed over time and removed by a clearing spin at 10,000 rpm for 10 min. The release profile was studied by taking aliquots of the sample over a period of 7 days; the amount of drug in the sample was then determined using ICP-OES (see below).

UV/visible Spectroscopy

CPMV concentration was determined using a NanoDrop 2000 Spectrophotometer (Thermo Scientific) with the reported extinction coefficient for CPMV ($\varepsilon_{260\ nm}$ = 8.1 mg^{-1} mL cm^{-1}).

Inductively Coupled Plasma Optical Emission Spectroscopy (ICP-OES)

Chromium content in CPMV was measured by ICP-OES (Agilent 730 Axial ICP-OES), as determined by the emission spectral line at 267.716 nm.

Transmission Electron Microscopy (TEM)

After sample dialysis, CPMV-Cr was imaged by TEM. Samples were diluted to a concentration of 0.1 mg/mL CPMV in deionized water then applied to a formvar/carbon-coated copper grid for 5 minutes. The grid was negatively stained with 2% (w/v) uranyl acetate for 2 minutes and imaged at 200 kV using a Zeiss Libra 200FE transmission electron microscope.

Cell Culture

Primary HASMC cultures (purchased from Cambrex) at passages 6–14 grown in DMEM/F12 media supplemented with 10% FBS and 1% penicillin-streptomycin (Cellgro) were used in all experiments. Confluent cells were placed in low glucose (5 mM)-0.2% FBS DMEM overnight (16–17 h) followed by incubation with 25 mM glucose in the presence or absence of 100 nM $CrCl_3$-loaded CPMV nanoparticles.

Immunocytochemistry

About 70% confluent HASMCs grown on cover slips in six-well clusters were treated as described above. Cells were fixed in a solution containing 4% paraformaldehyde and 0.2% Triton X-100 for 20 min at 25°C and blocked in 5% donkey serum for 1 h at room temperature. This was followed by overnight incubation at 4°C with rabbit anti-CPMV primary antibody (Pacific Immunology) or no primary antibody (used as negative control). Cells were then incubated with Alexa Fluor® 594 secondary antibody (1:1500) for 1 h at room temperature followed by washing in PBS (3X, 5 mins each). Cover slips were mounted using DAPI-containing vectashield mounting media (Vector Lab) for identification of cell nuclei. The mean red fluorescence intensity indicative of CPMV staining was measured for each image.

Proliferation of Cultured Smooth Muscle Cells

Primary HASMC cultures were plated (1500–2000 cells/well) on 96-well tissue culture plates in 10% FBS and 1% penicillin-streptomycin containing DMEM/F12 media. After allowing for overnight cell growth, HASMCs were treated with 25 mM glucose in presence or absence of 100 nM $CrCl_3$-loaded CPMV. Cell incubations were continued for 72 hours followed by measurement of cellular proliferation using WST-1 reagent (Cayman Chemicals), as we previously reported.[17]

Preparation of Whole Cell Lysate and Immunoblotting

Whole cell lysates were prepared and proteins were measured (BioRad), as we reported earlier.[17] Equal amounts of proteins were resolved on 8% SDS-polyacrylamide gels and transferred on PVDF membranes. Membranes were blocked in 5% nonfat dry milk for 45 mins-1 h at room temperature followed by overnight incubation at 4°C with different antibodies: anti-PCNA (1:300, Abcam), anti-phospho-Akt (1:1000, Cell Signaling), anti-total-Akt (1:1000, Cell Signaling), anti-phospho- and total-p38 (1:500, Cell Signaling), anti-TSP-1, (1:500; clone AB11, Thermo Fisher), anti-TGF-β (1:250, Bioss), anti-NF-κB (1:500, Bioss) and anti-β-actin (loading control, Cell Signaling). Equal protein loading was also confirmed by staining membranes with Ponceau S. Densitometric quantifications were conducted using ImageJ and Adobe photoshop softwares and results were expressed as fold-increase vs. Controls.

Lipid Uptake Assay

About 60–70% confluent HASMC cultures, seeded on cover slips in six-well plates, were placed overnight in serum-free low-glucose (5 mM) DMEM media. This was followed by the addition of 25 mM glucose and cell incubations were continued in presence or absence of 100 nM $CrCl_3$-loaded CPMV for 19 h; ox-LDL (50 μg/ml) was then added to the media and incubations were continued for an addition 4–5 h. Following this, media was aspirated and cells were rinsed in PBS followed by formalin fixation for 10 mins; cells were rinsed once again in PBS (1 min) and 60% isopropanol (15 sec). This was followed by staining of cells with (0.5%) Oil Red O solution for 15 mins at room temperature; cells were destained with 60% isopropanol for 15 sec followed by PBS washing. Nuclei were stained with Harris hematoxylin and cover slips were mounted on glycerin jelly. Images were acquired using Olympus BX40 microscope at 40X magnification.

Statistical Analyses

All experiments were repeated three-to-five times with two replicates for each treatment within an independent experiment. For microscopic experiments, six to ten images were collected for each individual treatment within each independent experiment. Images were quantified using ImageJ software. Results are presented as fold-increase vs. controls. Values are means ± SEM. Significant differences between the mean values were determined using unpaired Student's t test, with $p \leq 0.05$ being considered statistically significant.

Acknowledgments

This work was supported in parts by grants from Diabetes Action Research and Education Foundation (DAREF) award (to PR), Northeast Ohio Medical University start-up funds (to PR), National Institutes of Health NHLBI R21 HL121130 (to NFS) and NHLBI F31 HL129703 (to AMW).

References

1. Lusis AJ. Atherosclerosis. Nature. 2000; 407:233–241. [PubMed: 11001066]
2. Haffner SM, Mykkanen L, Festa A, Burke JP, Stern MP. Insulin-resistant prediabetic subjects have more atherogenic risk factors than insulin-sensitive prediabetic subjects: implications for preventing coronary heart disease during the prediabetic state. Circulation. 2000; 101:975–980. [PubMed: 10704163]

3. Abate N. Obesity and cardiovascular disease. Pathogenetic role of the metabolic syndrome and therapeutic implications. J. Diabetes Complications. 2000; 14:154–174. [PubMed: 10989324]
4. Isomaa B, Almgren P, Tuomi T, Forsen B, Lahti K, Nissen M, Taskinen MR, Groop L. Cardiovascular morbidity and mortality associated with the metabolic syndrome. Diabetes Care. 2001; 24:683–689. [PubMed: 11315831]
5. Lau FC, Bagchi M, Sen CK, Bagchi D. Nutrigenomic basis of beneficial effects of chromium(III) on obesity and diabetes. Mol. Cell. Biochem. 2008; 317:1–10. [PubMed: 18636317]
6. Lee NA, Reasner CA. Beneficial effect of chromium supplementation on serum triglyceride levels in NIDDM. Diabetes Care. 1994; 17:1449–1452. [PubMed: 7882815]
7. Anderson RA. Chromium in the prevention and control of diabetes. Diabetes Metab. 2000; 26:22–27. [PubMed: 10705100]
8. Hummel M, Standl E, Schnell O. Chromium in metabolic and cardiovascular disease. Horm. Metab. Res. 2007; 39:743–751. [PubMed: 17952838]
9. Martin J, Wang ZQ, Zhang XH, Wachtel D, Volaufova J, Matthews DE, Cefalu WT. Chromium picolinate supplementation attenuates body weight gain and increases insulin sensitivity in subjects with type 2 diabetes. Diabetes Care. 2006; 29:1826–1832. [PubMed: 16873787]
10. Mossop RT. Effects of chromium III on fasting blood glucose, cholesterol and cholesterol HDL levels in diabetics. Cent. Afr. J. Med. 1983; 29:80–82. [PubMed: 6883494]
11. Machalinski B, Walczak M, Syrenicz A, Machalinska A, Grymula K, Stecewicz I, Wiszniewska B, Dabkowska E. Hypoglycemic potency of novel trivalent chromium in hyperglycemic insulin-deficient rats. J. Trace Elem. Med. Biol. 2006; 20:33–39. [PubMed: 16632174]
12. Wang ZQ, Cefalu WT. Current concepts about chromium supplementation in type 2 diabetes and insulin resistance. Curr. Diab. Rep. 2010; 10:145–151. [PubMed: 20425574]
13. Jain SK, Lim G. Chromium chloride inhibits TNFalpha and IL-6 secretion in isolated human blood mononuclear cells exposed to high glucose. Horm. Metab. Res. 2006; 38:60–62. [PubMed: 16477544]
14. Jain SK, Kannan K. Chromium chloride inhibits oxidative stress and TNF-alpha secretion caused by exposure to high glucose in cultured U937 monocytes. Biochem. Biophys. Res. Commun. 2001; 289:687–691. [PubMed: 11726202]
15. Jain SK, Rains JL, Croad JL. High glucose and ketosis (acetoacetate) increases, and chromium niacinate decreases, IL-6, IL-8, and MCP-1 secretion and oxidative stress in U937 monocytes. Antioxid. Redox Signal. 2007; 9:1581–1590. [PubMed: 17665966]
16. Jain SK, Rains JL, Croad JL. Effect of chromium niacinate and chromium picolinate supplementation on lipid peroxidation, TNF-alpha, IL-6, CRP, glycated hemoglobin, triglycerides, and cholesterol levels in blood of streptozotocin-treated diabetic rats. Free Radic. Biol. Med. 2007; 43:1124–1131. [PubMed: 17854708]
17. Ganguly R, Sahu S, Chavez RJ, Raman P. Trivalent chromium inhibits TSP-1 expression, proliferation, and O-GlcNAc signaling in vascular smooth muscle cells in response to high glucose in vitro. Am. J. Physiol. Cell Physiol. 2015; 308:C111–C122. [PubMed: 25354527]
18. Lamson DW, Plaza SM. The safety and efficacy of high-dose chromium. Altern. Med. Rev. 2002; 7:218–235. [PubMed: 12126463]
19. Hathcock JN. Safety limits for nutrients. J. Nutr. 1996; 126:2386S–2389S. [PubMed: 8811802]
20. Rhodes MC, Hebert CD, Herbert RA, Morinello EJ, Roycroft JH, Travlos GS, Abdo KM. Absence of toxic effects in F344/N rats and B6C3F1 mice following subchronic administration of chromium picolinate monohydrate. Food Chem. Toxicol. 2005; 43:21–29. [PubMed: 15582192]
21. Katz SA, Salem H. The toxicology of chromium with respect to its chemical speciation: a review. J. Appl. Toxicol. 1993; 13:217–224. [PubMed: 8326093]
22. Eastmond DA, Macgregor JT, Slesinski RS. Trivalent chromium: assessing the genotoxic risk of an essential trace element and widely used human and animal nutritional supplement. Crit. Rev. Toxicol. 2008; 38:173–190. [PubMed: 18324515]
23. Manchester M, Singh P. Virus-based nanoparticles (VNPs): platform technologies for diagnostic imaging. Adv. Drug Deliv. Rev. 2006; 58:1505–1522. [PubMed: 17118484]

24. Wen AM, Wang Y, Jiang K, Hsu GC, Gao H, Lee KL, Yang AC, Yu X, Simon DI, Steinmetz NF. Shaping bio-inspired nanotechnologies to target thrombosis for dual optical-magnetic resonance imaging. J. Mater. Chem. B. 2015; 3:6037–6045.
25. Lewis JD, Destito G, Zijlstra A, Gonzalez MJ, Quigley JP, Manchester M, Stuhlmann H. Viral nanoparticles as tools for intravital vascular imaging. Nat. Med. 2006; 12:354–360. [PubMed: 16501571]
26. Plummer EM, Thomas D, Destito G, Shriver LP, Manchester M. Interaction of cowpea mosaic virus nanoparticles with surface vimentin and inflammatory cells in atherosclerotic lesions. Nanomedicine (Lond). 2012; 7:877–888. [PubMed: 22394183]
27. Steinmetz NF, Cho CF, Ablack A, Lewis JD, Manchester M. Cowpea mosaic virus nanoparticles target surface vimentin on cancer cells. Nanomedicine (Lond). 2011; 6:351–364. [PubMed: 21385137]
28. Steinmetz NF, Ablack AL, Hickey JL, Ablack J, Manocha B, Mymryk JS, Luyt LG, Lewis JD. Intravital Imaging of Human Prostate Cancer Using Viral Nanoparticles Targeted to Gastrin-Releasing Peptide Receptors. Small (Weinheim an der Bergstrasse, Germany). 2011; 7:1664–1672.
29. Wen AM, Shukla S, Saxena P, Aljabali AA, Yildiz I, Dey S, Mealy JE, Yang AC, Evans DJ, Lomonossoff GP, Steinmetz NF. Interior engineering of a viral nanoparticle and its tumor homing properties. Biomacromolecules. 2012; 13:3990–4001. [PubMed: 23121655]
30. Rae CS, Khor IW, Wang Q, Destito G, Gonzalez MJ, Singh P, Thomas DM, Estrada MN, Powell E, Finn MG, Manchester M. Systemic trafficking of plant virus nanoparticles in mice via the oral route. Virology. 2005; 343:224–235. [PubMed: 16185741]
31. Kaiser CR, Flenniken ML, Gillitzer E, Harmsen AL, Harmsen AG, Jutila MA, Douglas T, Young MJ. Biodistribution studies of protein cage nanoparticles demonstrate broad tissue distribution and rapid clearance in vivo. Int. J. Nanomedicine. 2007; 2:715–733. [PubMed: 18203438]
32. Singh P, Prasuhn D, Yeh RM, Destito G, Rae CS, Osborn K, Finn MG, Manchester M. Bio-distribution, toxicity and pathology of cowpea mosaic virus nanoparticles in vivo. J. Control. Release. 2007; 120:41–50. [PubMed: 17512998]
33. Gandra N, Abbineni G, Qu X, Huai Y, Wang L, Mao C. Bacteriophage bionanowire as a carrier for both cancer-targeting peptides and photosensitizers and its use in selective cancer cell killing by photodynamic therapy. Small. 2013; 9:215–221. [PubMed: 23047655]
34. Wen AM, Ryan MJ, Yang AC, Breitenkamp K, Pokorski JK, Steinmetz NF. Photodynamic activity of viral nanoparticles conjugated with C60. Chem. Commun. (Camb). 2012; 48:9044–9046. [PubMed: 22858632]
35. Lockney DM, Guenther RN, Loo L, Overton W, Antonelli R, Clark J, Hu M, Luft C, Lommel SA, Franzen S. The Red clover necrotic mosaic virus capsid as a multifunctional cell targeting plant viral nanoparticle. Bioconjug. Chem. 2011; 22:67–73. [PubMed: 21126069]
36. Lee DY, Lee H, Kim Y, Yoo SY, Chung WJ, Kim G. Phage as versatile nanoink for printing 3-D cell-laden scaffolds. Acta Biomater. 2016; 29:112–124. [PubMed: 26441128]
37. Wang J, Yang M, Zhu Y, Wang L, Tomsia AP, Mao C. Phage nanofibers induce vascularized osteogenesis in 3D printed bone scaffolds. Adv. Mater. 2014; 26:4961–4966. [PubMed: 24711251]
38. Zhao X, Lin Y, Wang Q. Virus-based scaffolds for tissue engineering applications. Wiley Interdiscip. Rev. Nanomed. Nanobiotechnol. 2015; 7:534–547. [PubMed: 25521747]
39. Koudelka KJ, Destito G, Plummer EM, Trauger SA, Siuzdak G, Manchester M. Endothelial targeting of cowpea mosaic virus (CPMV) via surface vimentin. PLoS Pathog. 2009; 5:e1000417. [PubMed: 19412526]
40. Steinmetz NF, Mauger J, Sheng H, Bensussan A, Marcic I, Kumar V, Braciak T. Two domains of vimentin are expressed on the surface of lymph node, bone and brain metastatic prostate cancer lines along with the putative stem cell marker proteins CD44 and CD133. Cancers. 2011; 3:2870–2885. [PubMed: 24212937]
41. Prasuhn DE Jr, Yeh RM, Obenaus A, Manchester M, Finn MG. Viral MRI contrast agents: coordination of Gd by native virions and attachment of Gd complexes by azide-alkyne cycloaddition. Chem. Commun. (Camb). 2007:1269–1271. [PubMed: 17356779]

42. Lindschau C, Quass P, Menne J, Guler F, Fiebeler A, Leitges M, Luft FC, Haller H. Glucose-induced TGF-beta1 and TGF-beta receptor-1 expression in vascular smooth muscle cells is mediated by protein kinase C-alpha. Hypertension. 2003; 42:335–341. [PubMed: 12939231]
43. Lizotte PH, Wen AM, Sheen MR, Fields J, Rojanasopondist P, Steinmetz NF, Fiering S. In situ vaccination with cowpea mosaic virus nanoparticles suppresses metastatic cancer. Nat. Nanotechnol. 2015 in press.
44. Leong HS, Steinmetz NF, Ablack A, Destito G, Zijlstra A, Stuhlmann H, Manchester M, Lewis JD. Intravital imaging of embryonic and tumor neovasculature using viral nanoparticles. Nat. Protoc. 2010; 5:1406–1417. [PubMed: 20671724]
45. Yildiz I, Lee KL, Chen K, Shukla S, Steinmetz NF. Infusion of imaging and therapeutic molecules into the plant virus-based carrier cowpea mosaic virus: cargo-loading and delivery. J. Control. Release. 2013; 172:568–578. [PubMed: 23665254]
46. Steinmetz NF, Hong V, Spoerke ED, Lu P, Breitenkamp K, Finn MG, Manchester M. Buckyballs meet viral nanoparticles: candidates for biomedicine. J. Am. Chem. Soc. 2009; 131:17093–17095. [PubMed: 19904938]
47. Wen AM, Steinmetz NF. The aspect ratio of nanoparticle assemblies and the spatial arrangement of ligands can be optimized to enhance the targeting of cancer cells. Adv. Healthc. Mater. 2014; 3:1739–1744. [PubMed: 24729309]
48. Kaltgrad E, O'Reilly MK, Liao L, Han S, Paulson JC, Finn MG. On-virus construction of polyvalent glycan ligands for cell-surface receptors. J. Am. Chem. Soc. 2008; 130:4578–4579. [PubMed: 18341338]
49. Koudelka KJ, Rae CS, Gonzalez MJ, Manchester M. Interaction between a 54-kilodalton mammalian cell surface protein and cowpea mosaic virus. J. Virol. 2007; 81:1632–1640. [PubMed: 17121801]
50. Plummer EM, Thomas D, Destito G, Shriver LP, Manchester M. Interaction of cowpea mosaic virus nanoparticles with surface vimentin and inflammatory cells in atherosclerotic lesions. Nanomedicine. 2012; 7:877–888. [PubMed: 22394183]
51. Ivaska J, Pallari HM, Nevo J, Eriksson JE. Novel functions of vimentin in cell adhesion, migration, and signaling. Exp. Cell Res. 2007; 313:2050–2062. [PubMed: 17512929]
52. Nieminen M, Henttinen T, Merinen M, Marttila-Ichihara F, Eriksson JE, Jalkanen S. Vimentin function in lymphocyte adhesion and transcellular migration. Nat. Cell Biol. 2006; 8:156–162. [PubMed: 16429129]
53. Wang R, Li Q, Tang DD. Role of vimentin in smooth muscle force development. Am. J. Physiol. Cell Physiol. 2006; 291:C483–C489. [PubMed: 16571866]
54. Ise H, Kobayashi S, Goto M, Sato T, Kawakubo M, Takahashi M, Ikeda U, Akaike T. Vimentin and desmin possess GlcNAc-binding lectin-like properties on cell surfaces. Glycobiology. 2010; 20:843–864. [PubMed: 20332081]
55. Lacolley P, Regnault V, Nicoletti A, Li Z, Michel JB. The vascular smooth muscle cell in arterial pathology: a cell that can take on multiple roles. Cardiovasc. Res. 2012; 95:194–204. [PubMed: 22467316]
56. Rensen SS, Doevendans PA, van Eys GJ. Regulation and characteristics of vascular smooth muscle cell phenotypic diversity. Neth. Heart J. 2007; 15:100–108. [PubMed: 17612668]
57. Faries PL, Rohan DI, Takahara H, Wyers MC, Contreras MA, Quist WC, King GL, Logerfo FW. Human vascular smooth muscle cells of diabetic origin exhibit increased proliferation, adhesion, and migration. J. Vasc. Surg. 2001; 33:601–607. [PubMed: 11241133]
58. Rivard A, Andres V. Vascular smooth muscle cell proliferation in the pathogenesis of atherosclerotic cardiovascular diseases. Histol. Histopathol. 2000; 15:557–571. [PubMed: 10809377]
59. Cefalu WT, Hu FB. Role of chromium in human health and in diabetes. Diabetes Care. 2004; 27:2741–2751. [PubMed: 15505017]
60. Althuis MD, Jordan NE, Ludington EA, Wittes JT. Glucose and insulin responses to dietary chromium supplements: a meta-analysis. Am. J. Clin. Nutr. 2002; 76:148–155. [PubMed: 12081828]

61. Graf K, Xi XP, Yang D, Fleck E, Hsueh WA, Law RE. Mitogen-activated protein kinase activation is involved in platelet-derived growth factor-directed migration by vascular smooth muscle cells. Hypertension. 1997; 29:334–339. [PubMed: 9039124]
62. Muto A, Fitzgerald TN, Pimiento JM, Maloney SP, Teso D, Paszkowiak JJ, Westvik TS, Kudo FA, Nishibe T, Dardik A. Smooth muscle cell signal transduction: implications of vascular biology for vascular surgeons. J. Vasc. Surg. 2007; 45(Suppl A):A15–A24. [PubMed: 17544020]
63. Zhan Y, Kim S, Izumi Y, Izumiya Y, Nakao T, Miyazaki H, Iwao H. Role of JNK, p38, and ERK in platelet-derived growth factor-induced vascular proliferation, migration, and gene expression. Arterioscler. Thromb. Vasc. Biol. 2003; 23:795–801. [PubMed: 12637337]
64. Kanda Y, Nishio E, Kuroki Y, Mizuno K, Watanabe Y. Thrombin activates p38 mitogen-activated protein kinase in vascular smooth muscle cells. Life Sci. 2001; 68:1989–2000. [PubMed: 11388701]
65. Guo R, Li W, Liu B, Li S, Zhang B, Xu Y. Resveratrol protects vascular smooth muscle cells against high glucose-induced oxidative stress and cell proliferation in vitro. Med. Sci. Monit. Basic Res. 2014; 20:82–92. [PubMed: 24971582]
66. Tabas I, Garcia-Cardena G, Owens GK. Recent insights into the cellular biology of atherosclerosis. J. Cell. Biol. 2015; 209:13–22. [PubMed: 25869663]
67. Jain SK, Croad JL, Velusamy T, Rains JL, Bull R. Chromium dinicocysteinate supplementation can lower blood glucose, CRP, MCP-1, ICAM-1, creatinine, apparently mediated by elevated blood vitamin C and adiponectin and inhibition of NFkappaB, Akt, and Glut-2 in livers of zucker diabetic fatty rats. Mol. Nutr. Food Res. 2010; 54:1371–1380. [PubMed: 20306473]
68. Adams JC. Thrombospondins: multifunctional regulators of cell interactions. Annu. Rev. Cell Dev. Biol. 2001; 17:25–51. [PubMed: 11687483]
69. Bornstein P. Thrombospondins as matricellular modulators of cell function. J. Clin. Invest. 2001; 107:929–934. [PubMed: 11306593]
70. Raugi GJ, Mullen JS, Bark DH, Okada T, Mayberg MR. Thrombospondin deposition in rat carotid artery injury. Am. J. Pathol. 1990; 137:179–185. [PubMed: 1695483]
71. Sajid M, Hu Z, Guo H, Li H, Stouffer GA. Vascular expression of integrin-associated protein and thrombospondin increase after mechanical injury. J. Investig. Med. 2001; 49:398–406.
72. Riessen R, Kearney M, Lawler J, Isner JM. Immunolocalization of thrombospondin-1 in human atherosclerotic and restenotic arteries. Am. Heart J. 1998; 135:357–364. [PubMed: 9489988]
73. Miano JM, Vlasic N, Tota RR, Stemerman MB. Smooth muscle cell immediate-early gene and growth factor activation follows vascular injury. A putative in vivo mechanism for autocrine growth. Arterioscler. Thromb. 1993; 13:211–219. [PubMed: 8427857]
74. Pallero MA, Talbert Roden M, Chen YF, Anderson PG, Lemons J, Brott BC, Murphy-Ullrich JE. Stainless steel ions stimulate increased thrombospondin-1-dependent TGF-beta activation by vascular smooth muscle cells: implications for instent restenosis. J. Vasc. Res. 2010; 47:309–322. [PubMed: 20016205]
75. Bayraktar M, Dundar S, Kirazli S, Teletar F. Platelet factor 4, beta-thromboglobulin and thrombospondin levels in type I diabetes mellitus patients. J. Int. Med. Res. 1994; 22:90–94. [PubMed: 8020643]
76. Stenina OI, Krukovets I, Wang K, Zhou Z, Forudi F, Penn MS, Topol EJ, Plow EF. Increased expression of thrombospondin-1 in vessel wall of diabetic Zucker rat. Circulation. 2003; 107:3209–3215. [PubMed: 12810612]
77. Raman P, Krukovets I, Marinic TE, Bornstein P, Stenina OI. Glycosylation mediates up-regulation of a potent antiangiogenic and proatherogenic protein, thrombospondin-1, by glucose in vascular smooth muscle cells. J. Biol. Chem. 2007; 282:5704–5714. [PubMed: 17178709]
78. Wang S, Lincoln TM, Murphy-Ullrich JE. Glucose downregulation of PKG-I protein mediates increased thrombospondin1-dependent TGF-{beta} activity in vascular smooth muscle cells. Am. J. Physiol. Cell Physiol. 2010; 298:C1188–C1197. [PubMed: 20164378]
79. Chamberlain J. Transforming growth factor-beta: a promising target for anti-stenosis therapy. Cardiovasc. Drug Rev. 2001; 19:329–344. [PubMed: 11830751]
80. Yokoyama H, Deckert T. Central role of TGF-beta in the pathogenesis of diabetic nephropathy and macrovascular complications: a hypothesis. Diabet. Med. 1996; 13:313–320. [PubMed: 9162605]

81. Zhu Y, Usui HK, Sharma K. Regulation of transforming growth factor beta in diabetic nephropathy: implications for treatment. Semin. Nephrol. 2007; 27:153–160. [PubMed: 17418684]

82. Jeong IK, Oh da H, Park SJ, Kang JH, Kim S, Lee MS, Kim MJ, Hwang YC, Ahn KJ, Chung HY, Chae MK, Yoo HJ. Inhibition of NF-kappaB prevents high glucose-induced proliferation and plasminogen activator inhibitor-1 expression in vascular smooth muscle cells. Exp. Mol. Med. 2011; 43:684–692. [PubMed: 21975282]

83. Allahverdian S, Pannu PS, Francis GA. Contribution of monocyte-derived macrophages and smooth muscle cells to arterial foam cell formation. Cardiovasc. Res. 2012; 95:165–172. [PubMed: 22345306]

84. Llorente-Cortes V, Martinez-Gonzalez J, Badimon L. LDL receptor-related protein mediates uptake of aggregated LDL in human vascular smooth muscle cells. Arterioscler. Thromb. Vasc. Biol. 2000; 20:1572–1579. [PubMed: 10845874]

85. Basford JE, Moore ZW, Zhou L, Herz J, Hui DY. Smooth muscle LDL receptor-related protein-1 inactivation reduces vascular reactivity and promotes injury-induced neointima formation. Arterioscler. Thromb. Vasc. Biol. 2009; 29:1772–1778. [PubMed: 19729608]

86. Llorente-Cortes V, Otero-Vinas M, Sanchez S, Rodriguez C, Badimon L. Low-density lipoprotein upregulates low-density lipoprotein receptor-related protein expression in vascular smooth muscle cells: possible involvement of sterol regulatory element binding protein-2-dependent mechanism. Circulation. 2002; 106:3104–3110. [PubMed: 12473559]

87. Cho CF, Shukla S, Simpson EJ, Steinmetz NF, Luyt LG, Lewis JD. Molecular targeted viral nanoparticles as tools for imaging cancer. Methods Mol. Biol. 2014; 1108:211–230. [PubMed: 24243252]

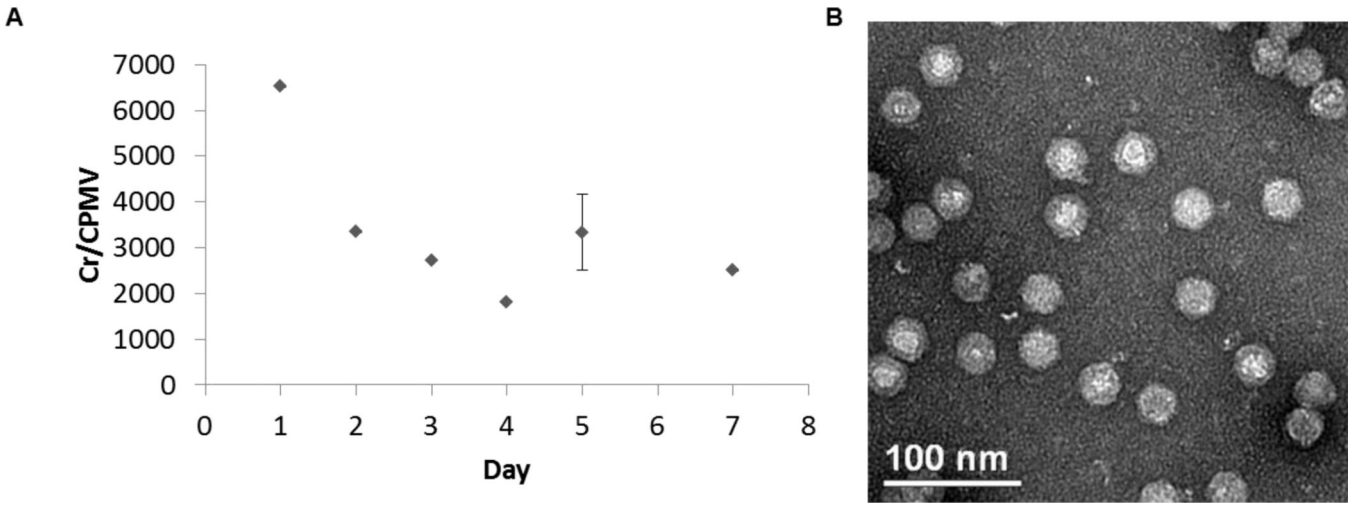

Figure 1. Loading and release of chromium in CPMV

A) After CPMV incubation with 50 mM $CrCl_3$, dialysis was performed against 10 mM HEPES with 10 mM EDTA. Quantification of chromium in CPMV-Cr over time was measured by ICP-OES. Error bars show standard deviation of three measurements (it should be noted that all data points were measured in triplicates and error bars are shown for each time point, significant experimental variation was only observed for data collected on day 5). B) Transmission electron microscopy of CPMV loaded with $CrCl_3$ indicated that the particle structure remains unchanged after modification.

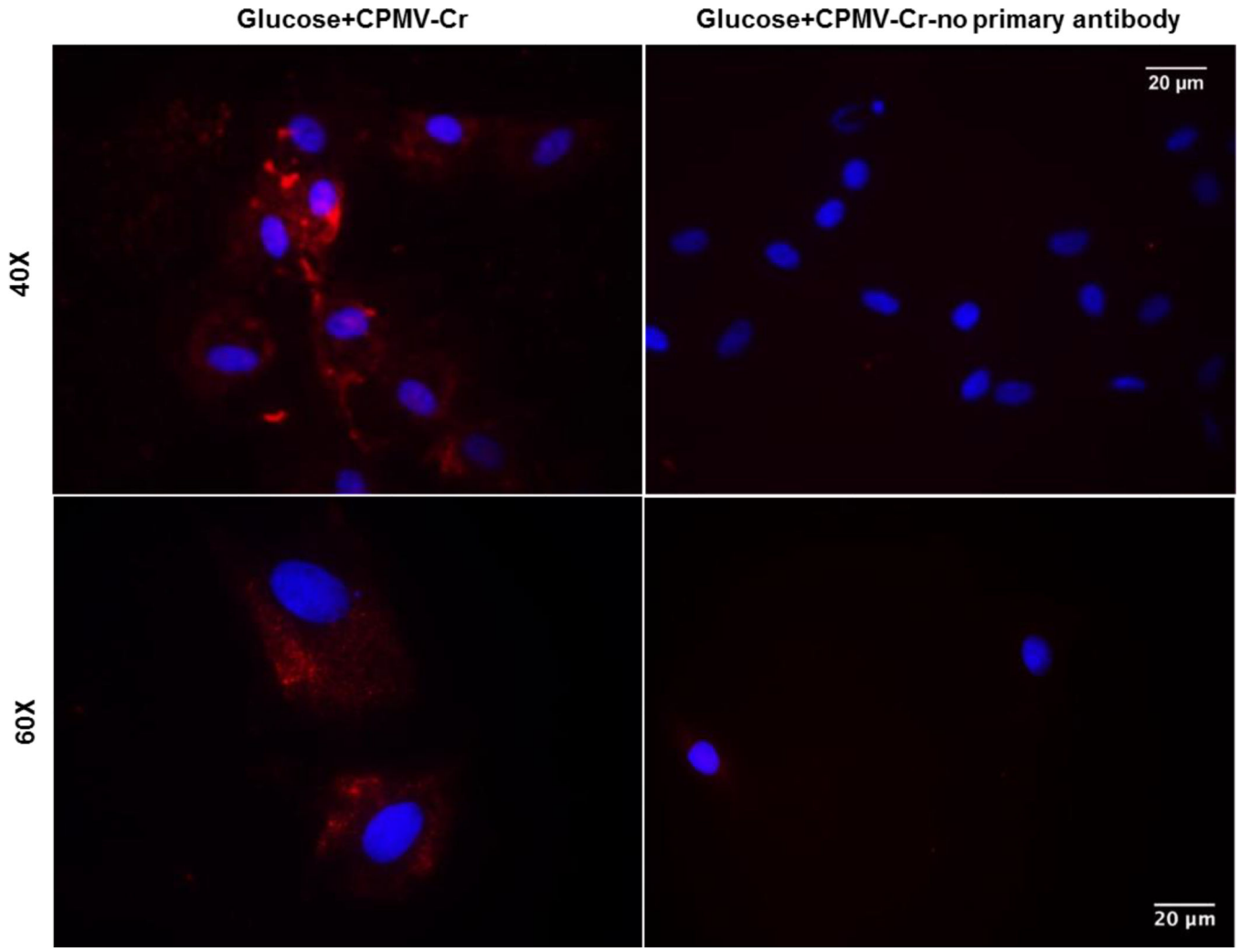

Figure 2. Uptake of $CrCl_3$-loaded CPMV nanoparticles by HASMCs *in vitro*

Primary HASMCs were grown on cover slips and acclimatized overnight in low glucose (5 mM) DMEM. Cells were incubated for 24 hrs with 100 nM $CrCl_3$-loaded CPMV nanoparticles in presence of 25 mM glucose. Fixed cells were incubated overnight with or without anti-CPMV primary antibody at 4°C followed by secondary incubation with Alexa Fluor® 555 conjugated anti-rabbit IgG for 1 h at room temperature. Shown are representative immunofluorescence images from three independent experiments. Images were captured at 40X (*upper panel*) and 60X (*lower panel*) magnification, depicting cytosolic CPMV staining (red) and DAPI (blue) stained nuclei.

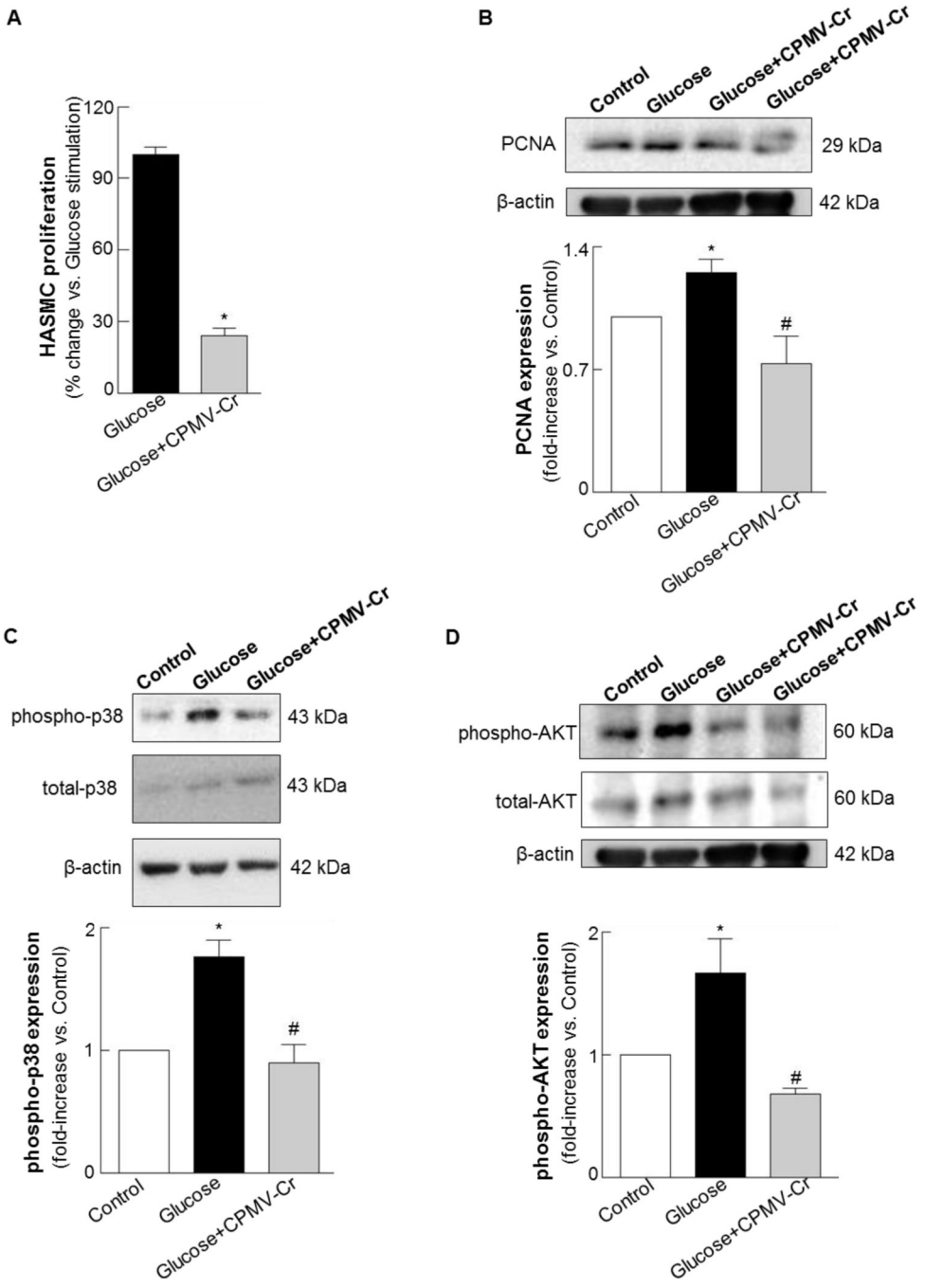

Figure 3. $CrCl_3$-loaded CPMV attenuates HASMC proliferation, inhibits PCNA, p38 and pAKT expression in glucose-stimulated HASMC

A) Primary HASMCs were grown in 96-well plates and incubated in 25 mM glucose containing serum free DMEM in presence or absence of 100 nM CPMV-Cr. Cell proliferation was assessed 72 h later using WST-1 reagent as described in Methods. Results are expressed as fold-change vs. glucose stimulation. Values are expressed as means ± S.E. (n=3–4); $^{*}p \leq 0.05$ vs. Glucose. B-D) Following overnight pre-incubation in low glucose (5 mM)-0.2% FBS-containing DMEM, primary HASMC cultures were incubated in 25 mM glucose with or without 100 nM $CrCl_3$-loaded CPMV nanoparticles for 24 hrs. Whole cell

lysates were prepared at endpoint and subjected to immunoblotting, as described in Methods. Shown are representative immunoblots depicting (B) PCNA, (C) p38 and (D) pAkt protein expression (*upper panels*); densitometric quantification of immunoblots from 3–5 independent experiments is shown in the bar graphs (*lower panels*). Results are expressed as fold-increase vs. Controls. All values are expressed as means ± S.E. (n=3–5); $^{*}p \leq 0.03$ vs. Control, $^{\#}p \leq 0.03$ vs. Glucose.

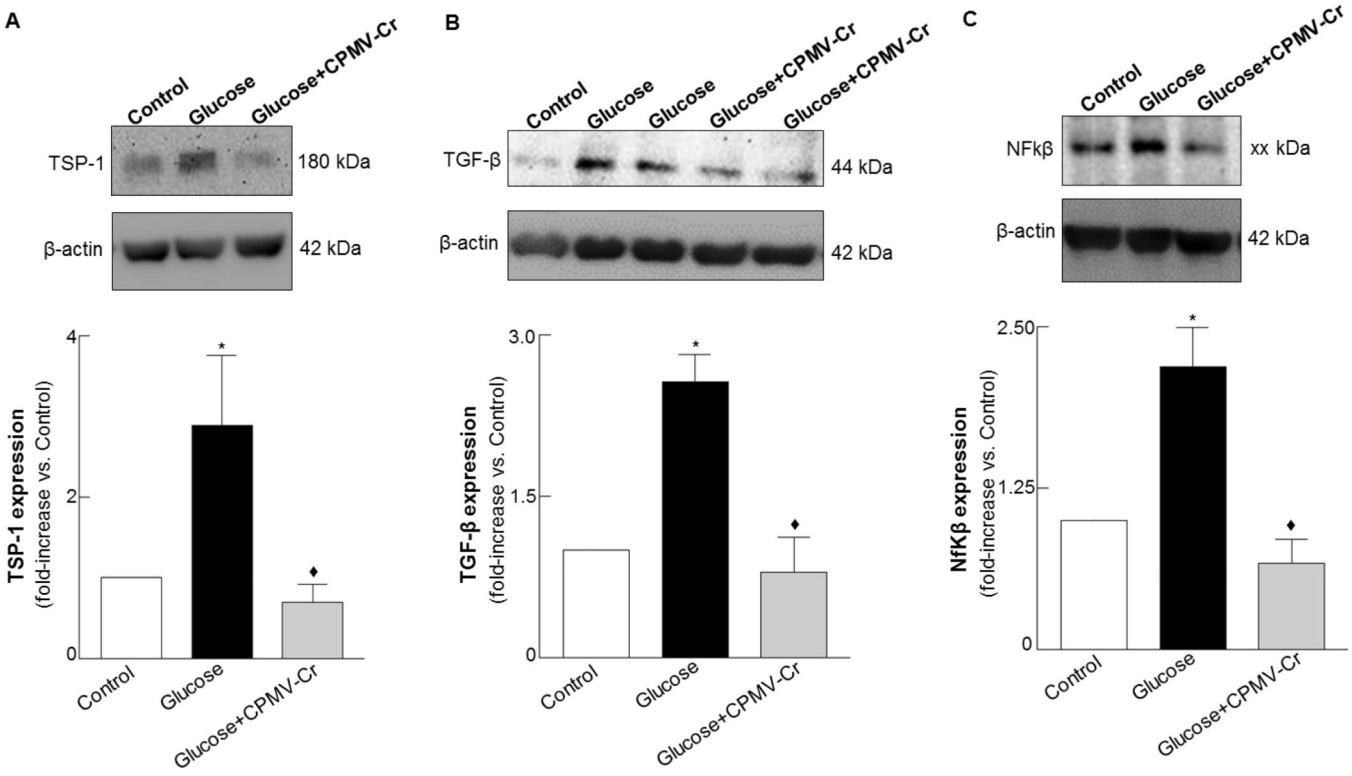

Figure 4. $CrCl_3$-loaded CPMV attenuates TSP-1, TGF-β and NF-kB expression in glucose-stimulated HASMC

Primary HASMC cultures were acclimatized overnight in low glucose (5 mM)-0.2% FBS-containing DMEM. This was followed by stimulation with 25 mM glucose in presence or absence of 100 nM $CrCl_3$-loaded CPMV nanoparticles for 24 hrs. For (B) cell incubation were continued for 12 h. Whole cell lysates were prepared at end point and utilized in immunoblotting experiments using antibodies against TSP-1, TGF-β and NF-κB. Shown are the representative immunoblots (*upper panels*); densitometric quantification of immunoblots from 3–5 independent experiments are shown in the bar graphs (*lower panels*). Results are expressed as fold-increase vs. Controls. All values are expressed as means ± S.E. (n=3–5); $^{*}p \leq 0.026$ vs. Control, $^{\blacklozenge}p \leq 0.04$ vs. Glucose.

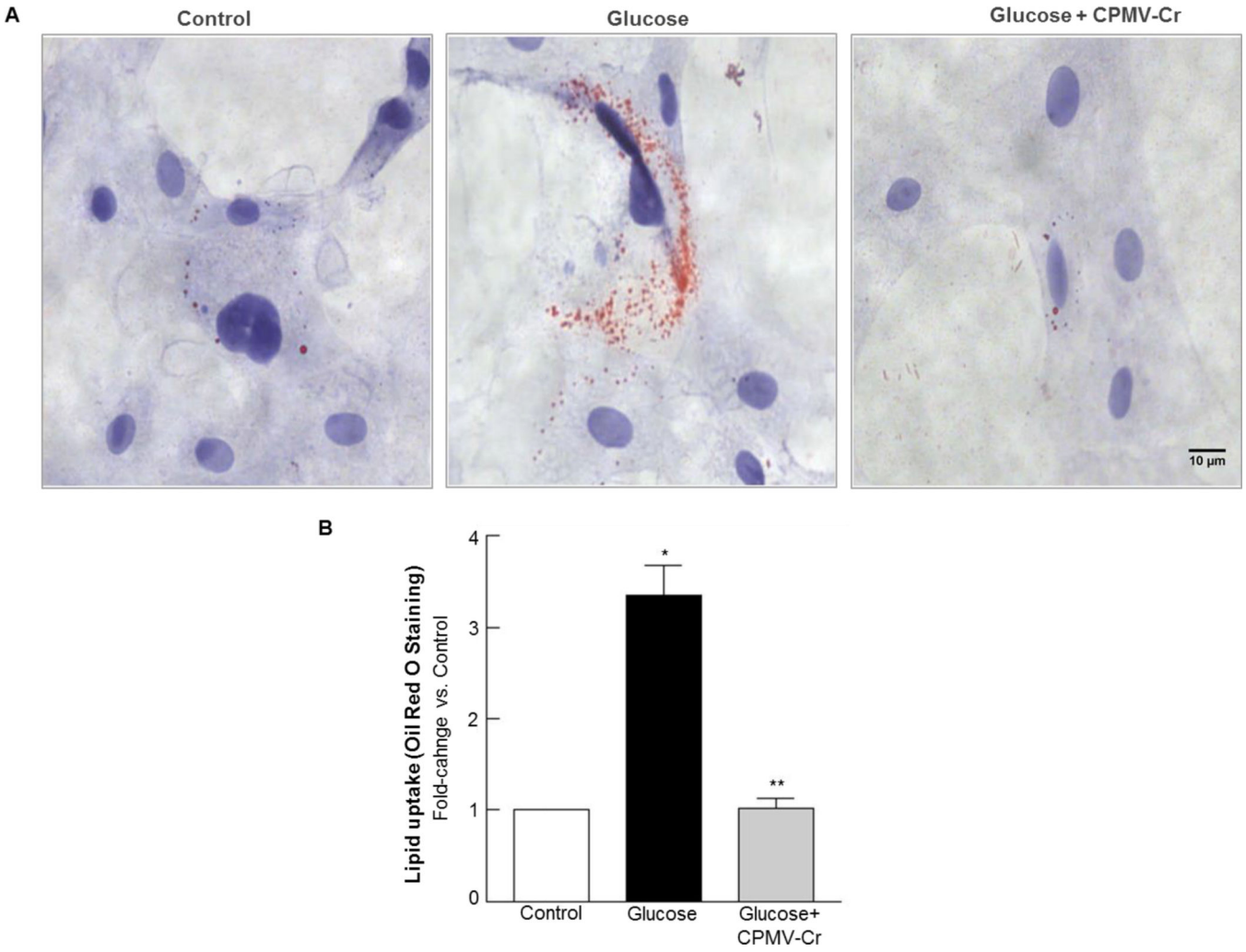

Figure 5. $CrCl_3$-loaded CPMV inhibits uptake of oxLDL in glucose-stimulated HASMC

A) Representative light microscopic images taken at 40X magnification showing Oil Red O stained oxidized LDL particles taken up by primary HASMCs and hematoxylin stained blue nuclei. HASMCs grown on cover slips were fixed and stained by Oil Red O followed by hematoxylin counter staining. B) Red intensity measurement from 10–20 different microscopic fields. Results are expressed as means ± S.E. (n=5); $^{*}p \leq 0.002$ vs. Control, $^{**}p \leq 0.0012$ vs. Glucose.